Solitary hypovascular hepatic nodules: comparison and differentiation between peripheral nodular cholangiocarcinoma and atypical liver hemangioma with MRI

Han Wang[1], Shengren Guo[2]

[1]Department of Ultrasound Medicine, Nanjing Drum Tower Hospital, The Affiliated Hospital of Nanjing University Medical School, Nanjing, China; [2]Department of Radiology, The Second Affiliated Hospital of Soochow University, Suzhou, China

Contributions: (I) Conception and design: H Wang; (II) Administrative support: Both authors; (III) Provision of study materials or patients: S Guo; (IV) Collection and assembly of data: Both authors; (V) Data analysis and interpretation: H Wang; (VI) Manuscript writing: Both authors; (VII) Final approval of manuscript: Both authors.

Correspondence to: Shengren Guo, MD, PhD. Department of Radiology, The Second Affiliated Hospital of Soochow University, 1055 Sanxiang Street, Suzhou 215008, China. Email: soochow_001@163.com; gshrgcl@21cn.com.

Background: Peripheral nodular cholangiocarcinoma (PCC) and hepatic hemangioma (HG) significantly differ in treatment strategies and prognosis. However, they can present similar imaging characteristics, making them difficult to distinguish. The distinction between PCC and atypical HG using pre-operative dynamic contrast-enhanced magnetic resonance imaging (DCE-MRI) holds substantial significance.

Methods: Fifty-four cases of solitary hypovascular hepatic nodules (nodules ≤3 cm in diameter and enhancement not exceeding the hepatic parenchyma) confirmed pathologically were collected, including 25 cases of PCC and 29 cases of HG. The clinical and DCE-MRI features were observed, and the apparent diffusion coefficient (ADC) values were compared. The *t*-test or Fisher's exact test was used to compare the differences between the two groups. Receiver operating characteristic (ROC) curve analysis was performed on the diagnostic results of the two readings before and after the study by three diagnostic physicians.

Results: The signal of PCC was more heterogeneous and could be shown as a ring hyperintensity signal on diffusion weighted imaging (DWI). The T2-weighted imaging (T2WI) signal of HG lesions showed a more homogeneous high-intense signal. The ADC value of PCC patients was lower than that of HG patients. Most of the patients in the two groups presented marginal enhancement in the arterial phase with infrequent abnormal perfusion around. The intratumoral vascular traversal signs in the PCC group showed a diagnostic significance. Among the lesions with marginal enhancement at arterial stage, the enhancement in PCC group was more likely to have annular enhancement with the main manifestation of delay reduction and nebulous or separated/astral center. On the other hand, HG tended to be more likely to have nodular enhancement in the arterial phase with delayed invariance at the margins and with no significant enhancement at the center. The area under the curves (AUC) of the three radiologists before and after the two readings were 0.645 and 0.888, respectively.

Conclusions: In the differentiation of PCC and atypical liver hemangioma, the presence of a circular hyper-intense signal in DWI, the ADC values, and the pattern and extent of enhancement of marginal and central lesions were of diagnostic significance.

Keywords: Peripheral nodular cholangiocarcinoma (PCC); atypical hepatic hemangioma; magnetic resonance imaging (MRI); the differential diagnosis

Introduction

There are huge differences in the therapeutic strategy and prognosis between cholangiocellular carcinoma and hemangioma. Since both can present as solitary hypovascular hepatic nodules, this poses a difficulty in differential diagnosis on imaging. To improve the accuracy of imaging diagnosis, the results of dynamic contrast-enhanced magnetic resonance imaging (DCE-MRI) and clinical data were collected from 54 cases of peripheral nodular cholangiocarcinoma (PCC) and atypical hepatic hemangioma (HG) patients with imaging manifestations of solitary hypovascular hepatic nodules. The characteristics of magnetic resonance imaging (MRI) plain scan and dynamic enhanced scan were analyzed and identified. We present this article in accordance with the STARD reporting checklist (available at https://tcr.amegroups.com/article/view/10.21037/tcr-23-27/rc).

Methods

Clinical materials

Retrospective analysis of patients who underwent surgery with pathologically confirmed cholangiocellular carcinoma

---

Highlight box

Key findings
- This article discusses the magnetic resonance imaging (MRI) features of peripheral nodular cholangiocarcinoma and atypical hepatic hemangioma in differential diagnosis.

What is known and what is new?
- Since both cholangiocellular carcinoma and hemangioma can present as solitary hypovascular hepatic nodules, this poses a difficulty in differential diagnosis on imaging.
- In the differentiation of peripheral nodular cholangiocarcinoma and atypical liver hemangioma, the presence of a circular hyper-intense signal in diffusion weighted imaging (DWI), the apparent diffusion coefficient (ADC) values, and the pattern and extent of enhancement of marginal and central lesions are of diagnostic significance.

What is the implication, and what should change now?
- In the cases of the peripheral nodular cholangiocarcinoma (PCC) and hepatic hemangioma (HG) with imaging of solitary hypovascular hepatic nodule, ADC value, MRI plain scan and the reinforcement model of the lesion including the edge and center under dynamic enhanced scan should be taken into consideration together, which would be promising to diagnose and identify the diseases.

---

and hemangioma admitted to the Second Affiliated Hospital of Soochow University from January 2018 to January 2022 with complete clinical data was performed. The study was conducted in accordance with the Declaration of Helsinki (as revised in 2013). The study was approved by the Institutional Review Board of the Second Affiliated Hospital of Soochow University (No. JD-HG-2023-46). The requirement for patient informed consent was waived as the retrospective nature of the study, which was carried out on the premise of protecting the privacy of patients. All patients received MRI plain scan and contrast-enhanced scan preoperatively. The imaging features of the patient were consistent with the diagnostic criteria of hypovascular hepatic nodules: (I) solitary nodules with diameters less than 3 cm; (II) according to the diagnostic criteria of hypovascular small hepatocellular carcinoma, those with non-enhancing or weakly enhancing lesion subjects in the arterial and portal phases were defined as hypovascular hepatic neoplasm (1). Based on the results of postoperative pathology, the patients were divided into two groups: PCC group and HG group.

MRI parameters

An MRI system (Intera Achieva 3.0 T; Philips Healthcare, Best, the Netherlands) was used. There were the following sequences in the baseline MRI: in-phase fast-field echo T1-weighted imaging (T1WI), breath-hold multishot T2-weighted imaging (T2WI), and respiratory-triggered heavily T2WI. Diffusion weighted imaging (DWI) images with B values of 0, 100, and 800 s/mm^2 were acquired simultaneously with respiratory-triggered single-shot echo-planar imaging. A monoexponential function with B values of 0 and 800 s/mm^2 was used to generate the apparent diffusion coefficient (ADC) map. Gadoxetic acid-enhanced imaging consisted of non-contrast agent-enhanced, arterial phase (20–35 s), portal phase (60 s), three-minute transitional phase, and 20-min hepatobiliary phase images. Three-dimensional fast-field echo sequences were used to obtain these images (high-resolution isotropic volume examination of T1, Philips Healthcare, Best, the Netherlands). A fluoroscopic bolus detection technique was used to determine arterial phase imaging time. By using a power injector, gadoxetic acid (Gd-EOB-DTPA, Primovist, Bayer Healthcare) was administered intravenously at 1–2 mL/s, followed by a 20 mL saline flush (0.025 mmol/kg). In order to reduce motion artifacts during the arterial phase, the contrast

material injection rate was reduced from 2 to 1 mL/s.

Image analysis

The images were evaluated by two radiologists with the qualification of an associate chief physician for reaching a consensus without prior knowledge of the pathological results. The following contents were mainly included: (I) general condition: the size, location, boundary of tumor, envelope depression sign, and intrahepatic bile duct dilatation. (II) Features of plain scan and measurement of ADC values: the signal characteristics of T1WI, T2WI and DWI were observed. ADC value of tumor parenchyma was measured by AD 4.3 workstation: the areas of interest were placed at the largest layer of the tumor, avoiding the areas such as cystic change, necrosis and hemorrhage. Three areas of interest were selected for each lesion, and the average value was taken. (III) Enhancement features of the focal arterial phase: observation of the arterial phase intensification performance, the presence of abnormal perfusion, and the presence of intratumoral vascular traversal signs. (IV) The lesions with circumferential and homogeneous intensification performance in the arterial phase were evaluated separately by subscripts: the degree of circumferential intensification and mode of intensification.

Analysis of the receiver operating characteristic (ROC) curves of the two pre- and post-reviews by physicians

The imaging diagnosis of the lesions was determined by three senior diagnostic physicians who read the films without knowing the pathological findings. After 2 weeks, the statistical results of the MRI signs in the two groups were presented to the three diagnostic physicians, and the second review was performed with the procedures same as before.

Statistical analysis

SPSS 24.0 software was used in this study. The independent sample t-test was used to analyze the quantitative data. Qualitative data were compared between groups using the χ^2 test and Fisher's exact probability method. $P<0.05$ was considered statistically significant. The judgement of the two benign and malignant lesions determined by the three diagnostic physicians was then analyzed by the ROC curve.

Results

Clinical materials

A total of 54 patients were collected, including 25 patients in the PCC group and 29 patients in the HG group.

PCC group (25 cases): 16 males and 9 females were included with a mean age of 57.24±13.688 years old. Eleven cases showed abdominal pain and abdominal discomfort as initial symptoms; ten cases were found through physical examination while two cases were accompanied by weight loss. There was an elevation of CA199 in one case, history of hepatitis B in two cases [one with increasing alpha fetoprotein (AFP)] as well as autoimmune hepatitis in one case. Thirteen cases were reported T1N0M0 and twelve cases were T2N0M0 in the light of preoperative staging. Laboratory examinations showed that the number of WBC slightly increased in three cases. One case with elevated AFP. Two cases with elevated carcinoembryonic antigen (CEA). Four cases with elevated C-reactive protein (CRP). Two cases with significantly elevated carbohydrate antigen 199 (CA199).

HG group (29 cases): 17 males and 12 females were included with a mean age of 49.62±16.439 years old. Four cases showed abdominal pain and abdominal discomfort as initial symptoms. Thirteen cases were found through physical examination. Laboratory examination showed that the number of WBC slightly increased in two cases. The levels of AFP and CEA were normal in 29 cases. The level of CRP was increased in two cases and the level of CA199 was slightly elevated to 46.7 U/mL in one case.

Image analysis

General characteristics

PCC group (25 cases): the mean diameter of the lesion was 15.800±7.963 mm. There were 15 cases with lesions located in the deep part of liver lobe and 10 cases with lesions under the liver capsule. Fifteen cases had a clear lesion boundary while ten cases had an unclear lesion boundary. Four of the cases with subcapsular lesions showed hepatic capsule retraction. Three cases were found intrahepatic cholangiectasis around the lesion. No cystic area, pseudo-pericardium, fatty degeneration and hemorrhagic signal were seen.

HG group (29 cases): the mean diameter of the lesion was 15.970±7.390 mm. There were 18 cases with lesions

Table 1 Results of comparison of general characteristics between PCC and HG

Observed content	PCC groups (n=25)	HG groups (n=29)	Statistics	P value
Gender			–	0.783
Male	16	17		
Female	9	12		
Age (years)	57.24±13.688	49.62±16.439	1.833	0.073
Diameter (mm)	15.800±7.963	15.970±7.390	−0.079	0.937
Lesion location			–	1.000
Sub-capsular of liver	10	11		
Underlying tissue	15	18		
Lesion boundary			–	0.394
Clear	15	21		
Unclear	10	8		
Hepatic capsule retraction			–	0.017
Exist	4	1		
No-exist	21	28		
Intrahepatic cholangiectasis			–	0.093
Exist	3	0		
No-exist	22	29		

Data are presented as No. or mean ± standard deviation. PCC, peripheral nodular cholangiocarcinoma; HG, hepatic hemangioma.

Table 2 Kappa test results

Observed content	Kappa value	P value
MRI signa	0.882	0.000
T1WI signal	1.000	0.000
T2WI signal	0.889	0.000
DWI signal	1.000	0.000
Arterial stage presentation	1.000	0.000
Marginal enhancement features of artery stage	0.957	0.000
Central enhancement features of artery stage	0.937	0.000
Marginal enhancement variation tendency	0.891	0.000
Central enhancement variation tendency	0.872	0.000
Abnormal perfusion	1.000	0.000
Intratumoral vascular transverse sign	1.000	0.000

MRI, magnetic resonance imaging; TIWI, T1-weighted imaging; T2WI, T2-weighted imaging; DWI, diffusion weighted imaging.

located in the deep part of the liver lobe and 11 cases with lesions under the liver capsule. Twenty-one cases had a clear lesion boundary while eight cases had an unclear lesion boundary. One of the cases with subcapsular lesions showed hepatic capsule retraction. No dilated bile ducts, cystic area, pseudo-pericardium, fatty degeneration and hemorrhagic signals were seen in any of the cases. There were no statistically significant differences in the general conditions of patients between PCC and HG (*Table 1*).

Kappa consistency test between two radiologists
The results of the consistency test were shown in *Table 2*.

MRI plain scan feature and ADC value
PCC group (25 cases): all of the cases manifested hypo-intense signals on T1WI. Eight of them manifested hyper-intense signals on T2WI, while seventeen of them presented equal hyper-intense signals on T2WI. Three of the 25 cases showed annular hyper-intense signals on DWI with an average ADC value of 1.513±0.246 (*Figure 1*).

HG group (29 cases): all of the cases manifested hypo-
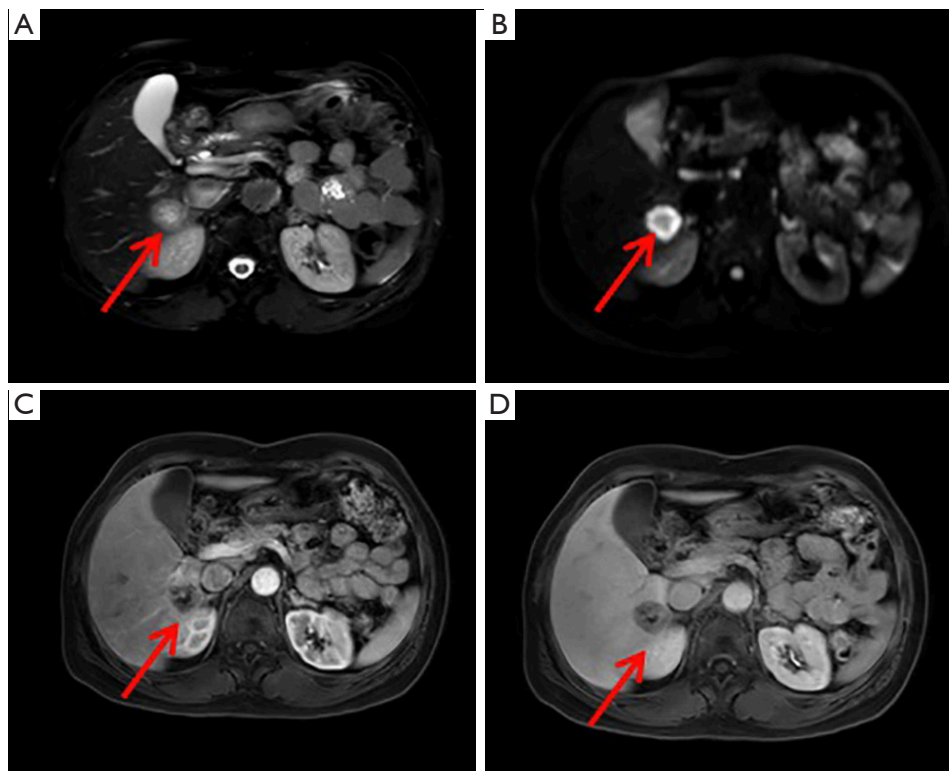
Figure 1 Postoperative pathology showed highly differentiated cholangiocarcinoma. The arrow points to the tumor. (A) T2WI of the lesion in the right lobe of the liver presented equal hyper-intense signal with unclear boundary. (B) DWI of the lesion presented annular high signal. (C,D) The margin of the lesion presented annular enhancement with the main manifestation of delay reduction. Abnormal perfusion and intratumoral vascular transverse sign was observed in the lesion. The main manifestation of the lesion centers was delay enhancement. T2WI, T2-weighted imaging; DWI, diffusion weighted imaging.

intense signals on T1WI. Nineteen of them manifested hyper-intense signals on T2WI while ten of them presented equal hyper-intense signals. All of the cases manifested homogeneous signal on DWI with an average ADC value of 1.836±0.470 (*Figure 2*).

There was no significant difference between the T1WI signals of PCC and HG compared with HG. PCC patients were heterogeneous and manifested annular hyper-intense signals on DWI. For T2WI, HG patients showed a relatively hyper-intense signal. The ADC values of PCC patients were lower than those of HG patients and the differences in the above features were statistically significant (*Table 3*).

Arterial stage presentation

PCC group (25 cases): in the arterial stage, 21 cases presented marginal enhancement while 4 cases presented uniform enhancement. Abnormal perfusion was observed in three cases and intratumoral vascular transverse sign was

observed in five cases.

HG group (29 cases): in the arterial stage, 26 cases presented marginal enhancement while 3 cases presented uniform enhancement. Abnormal perfusion was observed in one case. No intratumoral vascular transverse sign was observed in all lesions (*Figure 2*).

The majority of patients in the PCC and HG groups showed marginal enhancement in the arterial phase with little abnormal perfusion around the lesions. The differences between the two groups were not statistically significant. Compared with HG patients, the intratumoral vascular traversal signs in PCC group showed a diagnostic significance (*Table 3*).

Sub-items evaluation of marginal and uniform enhancement in the arterial phase

PCC group (21 cases): (I) among the four cases with uniform overall enhancement in arterial stage, two of
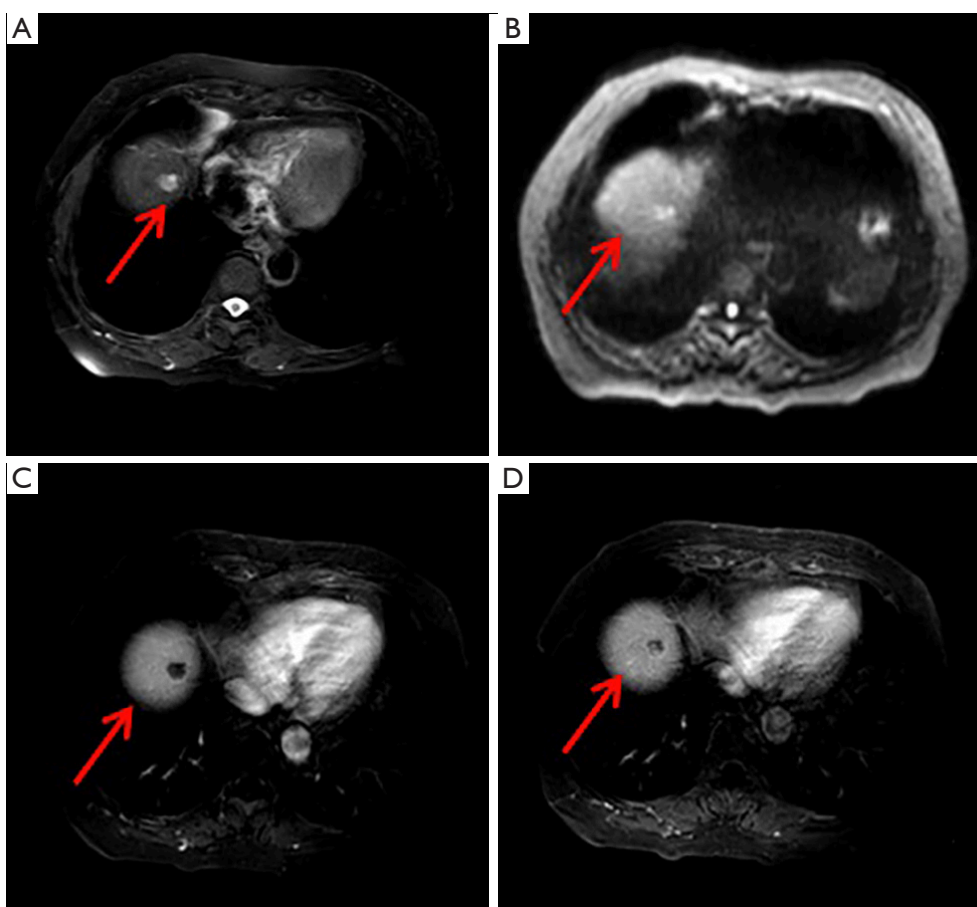
Figure 2 Postoperative pathology showed sclerosing angioma. The arrow points to the tumor. (A) T2WI of the lesion in the right lobe of the liver presented hyper-intense signal with unclear boundary; (B) DWI of the lesion presented slightly overall high signal; (C,D) the margin of the lesion presented annular enhancement with the main manifestation of delayed enhancement. The main manifestation of the lesion centers was delay enhancement as nodular. T2WI, T2 weighted imaging; DWI, diffusion weighted imaging.

them presented a delayed enhancement while one case presented delay invariable and attenuated respectively. (II) Of the 21 cases with marginal enhancement in arterial stage, 6 cases presented nodular enhancement while fifteen cases presented annular enhancement with the main manifestation of delay reduction. The main manifestation of the lesion centers was delay enhancement, which could be presented as nebulous, separated/astral and no enhancement in twelve cases, six cases and three cases respectively.

HG group (26 cases): (I) among the three cases with overall uniform enhancement in arterial stage, two of them presented delay enhancement while one case presented delay invariable. (II) Among the 26 cases with marginal enhancement in the arterial stage, seventeen presented nodular enhancement while nine presented annular enhancement with the main manifestation of delay

invariable. The main manifestation of the lesion centers was delay enhancement, which could be presented as nebulous, nodular and no enhancement in two cases, five cases and nineteen cases respectively.

There was no significant difference in the degree of enhancement of lesions with overall homogeneous enhancement between the PCC and HG groups in the arterial phase.

Among the lesions with marginal enhancement at arterial stage in both PCC and HG groups, the enhancement in PCC group was more likely to have annular enhancement, mainly showed delayed reduction and blurred or separated/stellate centers. On the other hand, the enhancement in HG group mainly showed nodular enhancement edges with unchanging delayed enhancement and centers with the absence of significant enhancement. The differences above

Table 3 Contrast results of MRI plain scan and contrast-enhanced scan between PCC and HG

Observed content	PCC groups (n=25)	HG groups (n=29)	Statistics	P value
MRI signal			–	0.001
Homogeneous	9	24		
Heterogeneous	16	5		
T1WI signal			–	1.000
Hypo-intense	25	29		
Equal-intense	0	0		
T2WI signal			–	0.001
Hyper-intense	8	19		
Equal hyper-intense	17	10		
DWI signal			–	0.093
Annular hyper-intense	3	0		
Homogeneous	22	29		
ADC value ($\times 10^{-3}$ mm^2/s)	1.513±0.246	1.836±0.470	−3.088	0.003
Arterial stage presentation			–	0.692
Marginal enhancement	21	26		
Uniform enhancement	4	3		
Abnormal perfusion			–	0.326
Exist	3	1		
No-exist	22	28		
Intratumoral vascular transverse sign			–	0.017
Exist	5	0		
No-exist	20	29		

Data are presented as No. or mean ± standard deviation. MRI, magnetic resonance imaging; TIWI, T1 weighted imaging; T2WI, T2 weighted imaging; DWI, diffusion weighted imaging; ADC, apparent diffusion coefficient; PCC, peripheral nodular cholangiocarcinoma; HG, hepatic hemangioma.

were statistically significant. However, patients in both PCC and HG groups showed delayed enhancement of the focal centers, with no statistically significant difference (*Table 4*).

ROC curve analysis of physicians

Three diagnostic physicians performed imaging diagnosis twice before and after learning the conclusions of the study. The area under the ROC curve (AUC) of the first diagnosis was 0.645 with a sensitivity and specificity of diagnosis of 60.0% and 69.0% respectively. The AUC of the second diagnosis was 0.888 after the training, with a sensitivity of 88.0% and a specificity of 89.7% for the lesions (*Figure 3*).

Discussion

PCC patients in this study were slightly older and some were accompanied by loss of weight, chronic hepatic diseases or abnormal levels of laboratory examination indicators. While in the HG group, the laboratory examination indicators of patients were generally in the normal range. However, as has been reported in the literature, due to the small extent of the lesions, the clinical symptoms and laboratory test results are atypical, making identification difficult (2).

PCC originates from peripheral capillary bile ducts which has relatively small diameter and mostly belong to

Table 4 Contrast results of MRI contrast-enhanced scan between PCC and HG with marginal enhancement

Observed content	PCC groups (n=21)	HG groups (n=26)	Statistics	P value
Marginal enhancement features of artery stage			–	0.019
Nodular	6	17		
Annular	15	9		
Central enhancement features of artery stage			30.019	0.000
Nebulous	12	2		
Separated/astral	6	0		
Nodular	0	5		
No enhancement	3	19		
Marginal enhancement variation tendency			–	0.000
Delayed enhancement	1	8		
Delay reduction	12	0		
Delay invariable	8	18		
Central enhancement variation tendency			0.948	0.793
Delayed enhancement	16	17		
Delay reduction	2	5		
Delay invariable	3	4		

MRI, magnetic resonance imaging; PCC, peripheral nodular cholangiocarcinoma; HG, hepatic hemangioma.
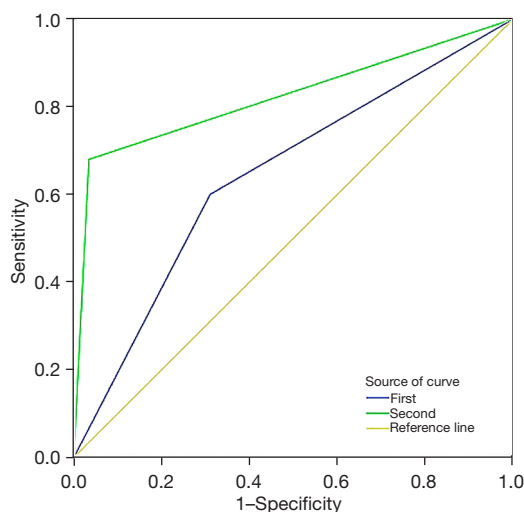
Figure 3 Analysis of ROC. The AUCs of the three diagnostic physicians was 0.645 in the first time and 0.888 in the second time. ROC, receiver operating characteristic curve; AUC, area under curves.

T1N0M0 or T2N0M0 phase (3). In the view of histology, the neoplasm of intrahepatic cholangiocarcinoma is mainly composed of fibrous tissue, malignant tumor cells and necrotic tissue (4). The fibrous tissue and malignant tumor manifest hypo-intense signals on T1WI and T2WI. The coagulation necrosis manifests hypo-intense or mixed signal on T1WI and hyper-intense or mixed signal on T2WI (5). When the tumor presents hemorrhage and necrosis, the signal on T1WI may be hypo-intense or mixed, and the signal on T2WI may be hyper-intense or mixed (6). Some cases are also found with signs of intrahepatic biliary cysts and hepatic capsule contraction. The typical signs of bile duct carcinoma are not obvious due to the small diameter of the lesion, making it difficult to be differentiated from hemangioma (7). In this study, PCC presented solitary hepatic nodules with clear or unclear boundaries, as well as relatively equal hypo-intense T1WI and slightly hyper-intense T2WI signals. Among them, the inhomogeneous signals were mainly derived from coagulative necrotic and

fibrous tissue.

Cavernous hemangioma consists of plenty of dilated sinuses covered by a monolayer of flattened endothelial cells. According to MRI report, HG presents with a homogeneous hyper-intense signal on T2W1 similar to cerebrospinal fluid (CSF), which is known as the bulb sign (8). Even in hypovascular hemangioma, this bulb sign was found in 19 patients in this study. The atypical presentation and misdiagnosis of hepatic hemangioma are often associated with the following factors: (I) morphological and anatomical changes, such as central scar, the internal septum, calcification, degenerated cysts, hemorrhage, retracted hepatic capsule and the expanded bile duct. (II) Abnormal forms of reinforcement resulting from modifications in haemodynamic. (III) Chronic hepatic diseases, such as steatohepatitis and hepatic cirrhosis (9). (IV) Effects of scanning operations, including partial volume effects and respiratory artifact (10). In this study, HG presented nodules of hypo-intense signals on T1WI and hypo-intense signals on T2WI, most of which had clear boundaries. Only one case showed a sign of a retracted hepatic capsule and no bile duct dilatation was observed in all cases.

DWI is the only method to measure and take image of the diffusion of water molecules *in vivo* to help diagnose disease by analyzing the diffusion changes of water molecules in the extracellular space and intracellularly under pathological conditions (11). ADC values reflect the tissue diffusion and perfusion which are related to the density of tumor cells. As the B value plays an important role in DWI technology, in this study, B value was set to 800 s/mm^2 for scanning and analyzing (11).

Cholangiocarcinoma is characterized by dense fibrous stromal components with obvious sclerosis in the centered tumor, low cell density, and active proliferation of cancer cells in the peripheral part, which give rise to a high circular signal on DWI (2,3).

ADC values of small hemangioma are influenced by the following conditions: (I) The faster the perfusion, the higher the ADC values. (II) Sclerosing hemangiomas with a large amount of fiber may exhibit low ADC values due to the limited water molecular dispersion. (III) Unlike ADC values, which can objectively reflect the dispersion of water molecules in tissue, the signal intensity of DWI is influenced by the rate of water diffusion in tissue and the T2 properties of the tissue itself. Therefore, despite having a high ADC value, hemangioma can show a relatively high signal in DWI due to the T2 penetration effect (11).

In this study, most of the small hypovascular angiomas were not problematic in terms of overall spread due to the presence of vascular lumen and the influence of blood flow and perfusion. On the other hand, the ADC value was higher than that of bile duct cell carcinoma, with statistically significant differences.

PCC is mainly manifested in the following aspects. Firstly, the lesions typically display mild homogenous or heterogeneous enhancement in the arterial phase. Corresponding to the pathological manifestations, a small or a medium amount of tumor cells are scattered or heterogeneously distributed in the lesion, mainly limited to necrosis and fibrous tissue. Moreover, there is often a circular enhancing edge in the arterial phase, which may be discontinuous with delayed enhancement. Reduction of enhancement in the margins is a characteristic sign of cholangiocellular carcinoma. The center of the lesion often appears cloudy and star-shaped, with a prolonged delayed phase contrary to pathological manifestation. The tumor cells are distributed at the edge of the lesion, with complete or incomplete circular enhancement or even and uneven thickness. The center may exhibit delayed enhancement, with a predominant component of fibrous tissue, while the necrotic tissue may not enhance. Star-shaped delayed enhancement scar is visible in the center of the lesion in six cases, indicating collagen scar formation or mucoid change (6). The final sign to note is vessel translocation. According to Kim *et al.*, this symptom occurs in around 53% of intrahepatic cholangiocarcinomas (12). In the present study, vascular displacement was found in five cases of PCC, whose pathological basis was tumor cell infiltration and infiltration into normal hepatic vessels.

As for HG, it can be manifested in the following aspects. In the first place, the lesions in the arterial stage present overall uniform and delayed enhancement. This hemangioma has a large vascular lumen, low hemodynamics, slow internal blood flow, and extremely slow perfusion and enhancement. Moreover, the relatively hypo-intense signal can be presented at every stage of lesion. The pathological manifestation is sclerosing hemangioma, which represents the terminal stage of the development of hemangioma (7). As the internal vascular space is gradually replaced by hyaline fibrous tissue, there is a reduction in the volume of the blood vessels, leading to a delayed uptake of contrast medium. These hemangiomas may lose their typical nodular enhancement and hyper-intense signal on T2WI due to the replacement of the internal vascular space with hyaline fibrous tissue. Additionally, they may

present lower ADC values on diffusion-weighted imaging due to limited diffusion of water molecules in the fibrous tissue. This can be useful in distinguishing these changes from active enhancing lesions. This volume reduction can cause the adjacent liver tissue to contract, leading to retraction of the liver capsule. Other than that, nodular peripheral enhancement is observed in most patients during the arterial phase, and the delayed enhancement remained unchanged. Meanwhile, the enhancement of the central area during the arterial phase is not apparent, but there might be an elevated enhancement in the delayed phase. The enhancement pattern observed is similar to that of typical hemangioma, but with the distinction that the predominant form of enhancement is due to the lack of blood supply. The dynamic enhancement pattern of the lesion depends on the size of the vascular lumen and the presence of fibrous scar tissue and other denatured components in the lesion. The large lumen contributes to slow blood flow and enhancement while the small lumen contributes to rapid blood flow and enhancement (13).

Finally, atypical hemangioma can be manifested as reverse filling the dynamic enhancement, which is related to a large number of vascular lacunae in the lesion center and fibrous components at peripheral region. Nonetheless, this enhancement pattern was not found in this study.

Conclusions

In summary, in the cases of solitary hypovascular hepatic nodules observed through imaging in PCC and HG, ADC value, MRI plain scan and the reinforcement model of the lesion including the edge and center under dynamic enhanced scan should be taken into consideration together for more accurate diagnosis and more effective disease identification.

Acknowledgments

Footnote

Reporting Checklist: The authors have completed the STARD reporting checklist. Available at https://tcr.amegroups.com/article/view/10.21037/tcr-23-27/rc

Data Sharing Statement: Available at https://tcr.amegroups.com/article/view/10.21037/tcr-23-27/dss

Peer Review File: Available at https://tcr.amegroups.com/article/view/10.21037/tcr-23-27/prf

Conflicts of Interest: Both authors have completed the ICMJE uniform disclosure form (available at https://tcr.amegroups.com/article/view/10.21037/tcr-23-27/coif). The authors have no conflicts of interest to declare.

Ethical Statement: The authors are accountable for all aspects of the work in ensuring that questions related to the accuracy or integrity of any part of the work are appropriately investigated and resolved. The study was conducted in accordance with the Declaration of Helsinki (as revised in 2013). The study was approved by the Institutional Review Board of the Second Affiliated Hospital of Soochow University (No. JD-HG-2023-46). The requirement for patient informed consent was waived due to the retrospective nature of the study.

References

1. Takayasu K, Arii S, Sakamoto M, et al. Clinical implication of hypovascular hepatocellular carcinoma studied in 4,474 patients with solitary tumour equal or less than 3 cm. Liver Int 2013;33:762-70.
2. Sheng RF, Zeng MS, Rao SX, et al. MRI of small intrahepatic mass-forming cholangiocarcinoma and atypical small hepatocellular carcinoma (≤3 cm) with cirrhosis and chronic viral hepatitis: a comparative study. Clin Imaging 2014;38:265-72.
3. Liang W, Wan D, Lu Q, et al. Dynamic enhancement patterns of small-diameter mass-forming intrahepatic cholangiocarcinomas on contrast-enhanced magnetic resonance imaging: Challenges faced by the radiologist. Medicine (Baltimore) 2017;96:e8351.
4. Zhou C, Wang Y, Ma L, et al. Combined hepatocellular carcinoma-cholangiocarcinoma: MRI features correlated

with tumor biomarkers and prognosis. Eur Radiol 2022;32:78-88.

5. Park S, Lee Y, Kim H, et al. Subtype Classification of Intrahepatic Cholangiocarcinoma Using Liver MR Imaging Features and Its Prognostic Value. Liver Cancer 2022;11:233-46.

6. Min JH, Kim YK, Choi SY, et al. Intrahepatic Mass-forming Cholangiocarcinoma: Arterial Enhancement Patterns at MRI and Prognosis. Radiology 2019;290:691-9.

7. Jia C, Liu G, Wang X, et al. Hepatic sclerosed hemangioma and sclerosing cavernous hemangioma: a radiological study. Jpn J Radiol 2021;39:1059-68.

8. Mamone G, Miraglia R. The "light bulb sign" in liver hemangioma. Abdom Radiol (NY) 2019;44:2327-8.

9. Mamone G, Di Piazza A, Carollo V, et al. Imaging of hepatic hemangioma: from A to Z. Abdom Radiol (NY) 2020;45:672-91.

10. Huang M, Zhao Q, Chen F, et al. Atypical appearance of hepatic hemangiomas with contrast-enhanced ultrasound. Oncotarget 2018;9:12662-70.

11. Gatidis S, Schmidt H, Martirosian P, et al. Apparent diffusion coefficient-dependent voxelwise computed diffusion-weighted imaging: An approach for improving SNR and reducing T2 shine-through effects. J Magn Reson Imaging 2016;43:824-32.

12. Kim YK, Han YM, Kim CS. Comparison of diffuse hepatocellular carcinoma and intrahepatic cholangiocarcinoma using sequentially acquired gadolinium-enhanced and Resovist-enhanced MRI. Eur J Radiol 2009;70:94-100.

13. Kim YY, Kang TW, Cha DI, et al. Gadoxetic acid-enhanced MRI for differentiating hepatic sclerosing hemangioma from malignant tumor. Eur J Radiol 2021;135:109474.